

# CFD Investigation of the Effects of Re-Entrant Combustion Chamber Geometry in a HSDI Diesel Engine

Raouf Mobasheri, Zhijun Peng

**Abstract**—A CFD simulation has applied to explore the effects of combustion chamber geometry on engine performance and pollutant emissions in a HSDI diesel engine. Three ITs (Injection Timing) at 2.65 CA BTDC, 0.65 CA BTDC and 1.35 CA ATDC, all with 30 crank angle pilot separations has firstly considered to identify the optimum IT for achieving the minimum amount of pollutant emissions. In order to investigate the effect of combustion chamber, thirteen different piston bowl configurations have been designed and analyzed. For all the studied cases, compression ratio, squish bowl volume and the amount of injected fuel were kept constant to assure that variation in the engine performance were only caused by geometric parameters. The results showed that by changing the geometric parameters on piston bowl, the amount of emission pollutants can be decreased while the other performance parameters of engine remain constant.

**Keywords**—HSDI Diesel Engine, Combustion Chamber Geometry, Pilot Injection, Injection Timing.

## I. INTRODUCTION

THE diesel engine has been proven to be a feasible solution for passenger cars in the European market and has great potential for the US market owing to its high fuel conversion efficiency, which can be 40 per cent more than that of modern spark ignition engines [1]-[3]. The current focus of engine research is on the simultaneous reduction in the soot and NO<sub>x</sub> to meet increasingly strict regulations, while maintaining reasonable fuel economy. Since the factors leading to NO<sub>x</sub> and soot emissions are totally different, it is very difficult to reduce them simultaneously. Another difficult problem is the fact that traditional methods for reducing one of these emissions are inclined to increase the other. In order to overcome this trade-off feature between NO<sub>x</sub> and soot emissions for future diesel engines, it is necessary to explore the vast design space using new analysis techniques. Optimization of current engine systems is the most economic and feasible way to achieve this aim, because it minimizes the required modifications to the whole vehicle system. Important design parameters include the injection timing, injection pressure, injection rate shape, nozzle design, swirl ratio, combustion chamber design, turbo charging, and exhaust gas recirculation (EGR).

Raouf Mobasheri is with the Mechanical Engineering, School of Engineering and Informatics, University of Sussex, Brighton, United Kingdom (Phone:+44-1273872562; e-mail: r.mobasheri@sussex.ac.uk).

Zhijun Peng is with the Mechanical Engineering, School of Engineering and Informatics, University of Sussex, Brighton, United Kingdom (Phone: +44-1273678928; e-mail: z.peng@sussex.ac.uk).

The effect of combustion chamber geometry on engine performance and exhaust emissions has been investigated by many researchers in the past [4]-[9], since with the proper combustion chamber design significant benefits can be achieved regarding the reduction of pollutant emissions, without affecting seriously the engine performance. The effect of combustion chamber shape on the engine performance is very complex due to its influence on the flow field and the air-spray interaction. The results in literature confirm that it is difficult to define an optimized combustion chamber, because of the influence of engine specification and injection system. From results in literature, Heywood [10] deduced that for a fixed compression ratio, the swirl levels at TDC increases if the bowl diameter is reduced, leading to less smoke, higher NO<sub>x</sub> levels and HC emissions. The squish-swirl interaction, instead, is influenced by the offset of the bowl with respect to the cylinder axis.

Saito et al. [4] performed an experimental study of bowl geometry in a small-bore diesel engine. Two open-type chambers were tried, one shallow and one deep. A re-entrant chamber was also tried, with equal maximum bowl diameter to the open chambers. The throat diameter of the re-entrant bowls was varied. They found that the re-entrant chamber produced shorter ignition delays, lower fuel consumption, and lower soot and NO<sub>x</sub> emissions when used with retarded injection timings. Bianchi et al. [5] performed a computational study on the use of a larger diameter, less re-entrant bowl configuration along with high pressure common rail fuel injection and low swirl in a small-bore diesel engine. The concept was to use a bowl design better suited to the modern injection system, thereby eliminating spray-wall impingement and the need for high swirl. This would increase the volumetric efficiency and possibly allow for simultaneous reductions in exhaust emissions and fuel consumption. The spray angle and number of injector holes was also changed. It was found that the high-pressure common rail injection system provided sufficient mixing without a highly re-entrant bowl and high swirl. De Risi et al. [6] performed a combined experimental and computational study on the effects of chamber geometry and engine speed on emissions in a small-bore diesel. The basic chamber shape investigated was a Mexican hat-type bowl. Five different variations of this shape were tried, one of which was an open-type bowl. They found the effect of bowl geometry more prevalent at low engine speeds. At higher engine speeds a smoother bowl lip resulted in lower soot and higher NO<sub>x</sub>. The best results were found

when aiming the fuel spray at the bottom of the bowl. Zhu et al. [7] studied the effects of the re-entrant lip shape of the piston bowl on a high speed direct injection (HSDI) diesel engine. The results have shown that a larger throat diameter bowl with narrow and high pip produces a lower ISFC because of better mixing in the bowl and soot emission due to lower soot formation in cylinder head region and higher soot oxidation due to high temperature.

It is well known that the spray characteristics must be well matched with the combustion chamber geometry and air motion to achieve optimal performance in a direct injection (DI) diesel engine. Pilot injection has been considered as another effective method for improvement the combustion and emission characteristics in DI Diesel engines [11]-[13]. While the injected fuel is split into two or more pulses, it can lead to an increase in the ignition delay with regard to the initial fuel pulse. Then a greater fraction of heat release will occur later in the expansion stroke. This helps to reduce the heat release rate of the premixed combustion and the result is lower NOx formation. Meanwhile, pilot injection enhances the fuel-air mixing, thus reducing soot forming regions significantly.

Zhang [11] investigated the effect of a pilot injection on NOx, soot emissions, and combustion noise in a small diesel engine. Soot emission was seen relevant to the pilot flame and reducing the pilot flame could reduce soot emissions. By optimizing the EGR rate, pilot timing and quantity, main timing, and dwell between the main and pilot injections, simultaneous reduction of NOx and PM was obtained in an HSDI diesel engine [12]. Another study on pilot injection was done by Tanaka et al. [13]. It was shown that simultaneous reduction of combustion noise and emissions is possible by decreasing the influence of the pilot burned gas through minimizing the fuel quantity and advancing the pilot injection timing.

While combustion chamber geometry and pilot injection have been suggested as two important factors to improve engine performance and amount of pollutant emission, it is of interest to explore the combined influence of their interaction on possibility of simultaneous reduction in particulate and NOx emission.

The objective of this paper is threefold: first, to investigate in detail the effects of the combustion chamber geometry on combustion and emission characteristics in an HSDI multi-injection diesel engine; then to model the combination of optimized geometries and different pilot injection timing; finally, to assess this combination to identify the best operating points.

## II. DESCRIPTION OF THE CFD MODEL

The CFD simulation in the present study has done by using the CFD Fire Code v2009.2 [14]. With the addition and modification of many sub-models, this code is now being widely applied and validated for engine combustion simulations [15], [16]. These models have been adequately described in the literature [14]-[23] and are only briefly described here.

The ECFM-3Z combustion model which is based on the Coherent Flame Model has been used for combustion modelling in this study. The ECFM-3Z (E stands for extended) model [17], [18] distinguishes between all three main regimes relevant in Diesel combustion, namely auto-ignition, premixed flame and non-premixed, i.e. diffusion combustion. The Shell auto-ignition model was used for modelling of the auto-ignition [19]. In this generic mechanism, 6 generic species for hydrocarbon fuel, oxidizer, total radical pool, branching agent, intermediate species and products were involved.

The standard WAVE model, described in [20]-[22] was used for the primary and secondary atomization modeling of the resulting droplets. In this model the growth of an initial perturbation on a liquid surface is linked to its wave length and to other physical and dynamic parameters of the injected fuel and the domain fluid. The Dukowicz model was applied for treating the heat-up and evaporation of the droplets, which is described in [23], [24]. This model assumes a uniform droplet temperature. In addition, the rate of droplet temperature change is determined by the heat balance, which states that the heat convection from the gas to the droplet either heats up the droplet or supplies heat for vaporization. A stochastic dispersion model was employed to take the effect of interaction between the particles and the turbulent eddies into account by adding a fluctuating velocity to the mean gas velocity [14]. This model assumes that the fluctuating velocity has a randomly Gaussian distribution. The spray wall interaction model used in the simulations was based on the spray-wall impingement model described in [21].

In this study, the  $k$ - $\zeta$ - $f$  model is used as default model for turbulence and turbulent wall heat transfer modeling. One of the main advantages of this model is its robustness to be used for computations involving grids with moving boundaries and highly compressed flows as it is the case in IC-engines. The mean reaction rate has been evaluated by means of the Coherent Flamelet Model (CFM) [18]. This model assumes that a droplet, which hits the wall is affected by rebound or reflection based on the Weber number.

The Extended Zeldowich mechanism [14] was used for prediction of NOx formation. In this study, soot emission is modelled by the Kennedy, Hiroyasu and Magnussen mechanism [25].

## III. ENGINE SPECIFICATION AND OPERATING CONDITIONS

The experimental data obtained from a four cylinders, high speed direct injection (HSDI) diesel engine were used for model validation in this study [26]. The specifications of the detailed engine and the fuel injection system are listed in Table I. The calculations were carried out for a part load operation at 1600 r/min without EGR. Note that in all figures and tables 360° CA corresponds to TDC position.

TABLE I  
ENGINE AND FUEL INJECTION SYSTEM SPECIFICATIONS

Ford diesel Engine	
Engine type	4-valve 2.0 L diesel engine
Number of cylinders	4
Bore	86.00 mm
Stroke	86.00 mm
Compression ratio	18.2:1
Connecting-rod length	160.00 mm
Squish height	0.86 mm
Piston shape	Re-entrant
IVC	143° CA BTDC
EVO	131° CA ATDC
Injection system	Common-rail system
Number of nozzle holes	6
Injector Hole Diameter	0.159 mm
Injector cone angle	154°, 130°, 120°
Total fuel	20.5 mg
Pilot fuel	0.5 mg
Pilot SOI	-35°, -30°, -25°, -20° CA ATDC
Pilot duration	1.21° CA
Main SOI	-0.65° CA ATDC
Main duration	10.45° CA

#### IV. COMPUTATIONAL DOMAIN

A 60° sector mesh of the combustion chamber considering the fuel injector with six holes was used to calculate combustion and emission characteristics. The computational mesh was created using AVL ESE Diesel Tool [14]. The computational grid at top dead centre (TDC) is shown in Fig. 1. Computations were performed from the intake valve close timing until the exhaust valve open timing. The ground of the bowl has been meshed with two continuous layers for a proper calculation of the heat transfer through the piston wall. The final mesh consists of a hexahedral dominated mesh. Number of cells in the mesh was about 61043 and 28453 at BDC and TDC, respectively. The present resolution was found to give adequately grid independent results.

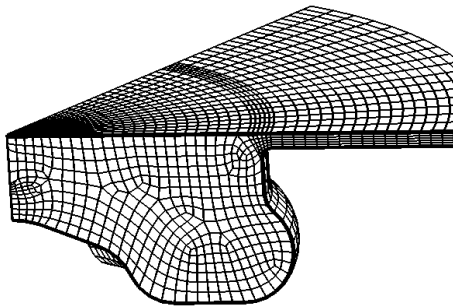


Fig. 1 Computational mesh at TDC

#### V. RESULTS AND DISCUSSION

##### A. Model Validation

In order to validate the accuracy of calculated results, the predicted results were compared with the experimental results.

Fig. 2 shows the comparison between the experimental and calculated in-cylinder pressures.

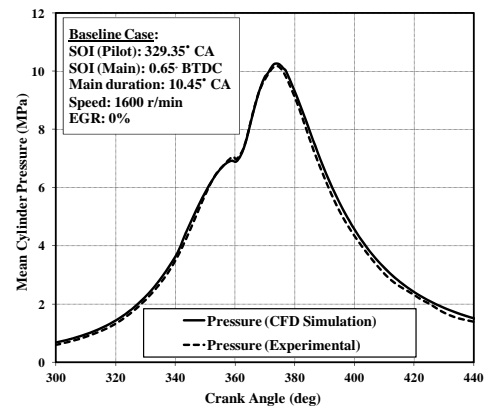


Fig. 2 Comparison between the experimental and calculated cylinder pressures

It is observed from Fig. 2 that during the whole part of the closed engine cycle, the calculated results show good agreement with the experimental results, implying that the combustion process is successfully modelled.

Fig. 3 illustrates the comparison between the experimental results and calculated emissions according to the crank angle. It can be seen that the calculated soot emission rapidly increased from the start of the combustion because combustion occurred in fuel-rich regions. After that, soot is decomposed or oxidized gradually during the expansion stroke. As illustrated in Fig. 3, the NOx and soot emissions trend was well predicted by the model.

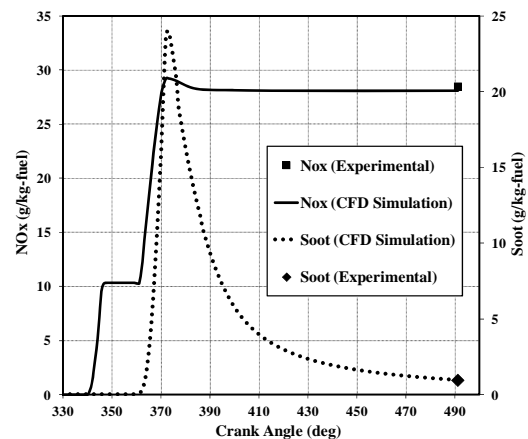


Fig. 3 Comparison between the experimental and calculated NOx and soot amounts

##### B. Effect of Injection Timing

Based on the confidence gained from validation, the study is extended to evaluate the prediction capability of the model to simulate the engine under different injection timings. For this purpose, three main injection timing, (1) 2.65 BTDC, (2) 0.65 BTDC and (3) 1.35 ATDC, all with 30 crank angle pilot

separations were used to investigate the effect of the injection timing on combustion characteristics and amount of pollutant emissions.

Figs. 4 and 5 show the in-cylinder averaged pressure and temperature profiles obtained for three injection timings.

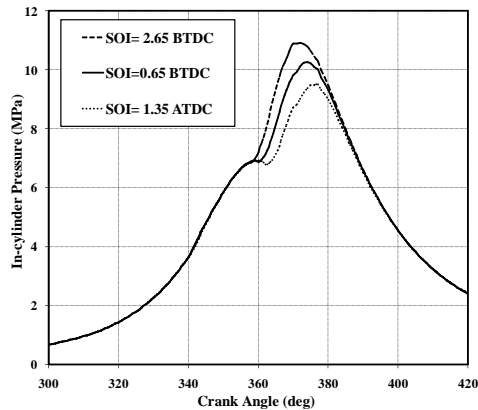


Fig. 4 Effect of the injection timing on the cylinder pressure

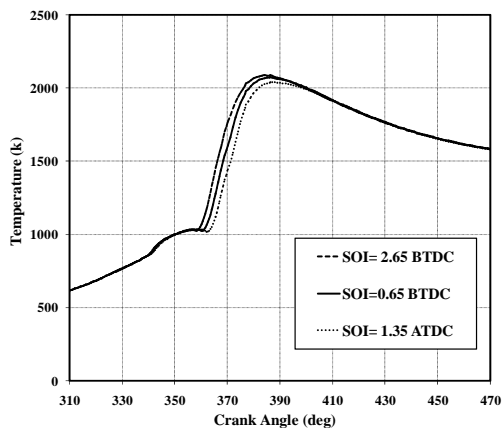


Fig. 5 Effect of the injection timing on the in-cylinder temperature

As illustrated in Figs. 4 and 5, the advanced injection timing demonstrates higher peak pressure and temperature and retarded injection timing shows lower in-cylinder pressure and temperature. As the injection timing is advanced, pressure and temperature within the cylinder is not sufficient to ignite the fuel as a result a large amount of evaporated fuel is accumulated during the ignition delay period. However, in the case of retarded injection timing, pressure and temperature inside the cylinder is sufficient to ignite the fuel and a relatively small amount of evaporated fuel is accumulated during the ignition delay period.

Figs. 6 and 7 show the heat release rate and accumulated heat release, respectively.

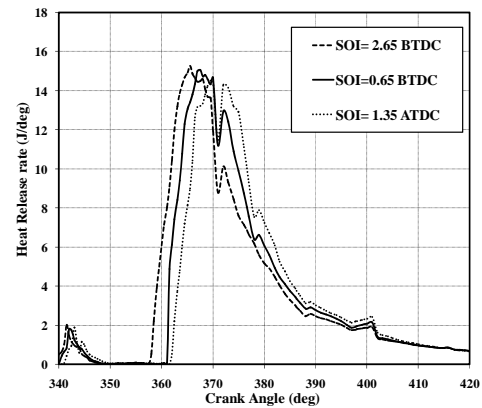


Fig. 6 Effect of the injection timing on heat release rate

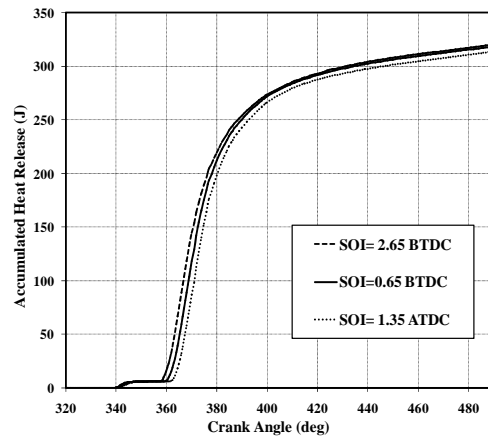


Fig. 7 Effect of the injection timing on accumulated heat release

As illustrated in Figs. 6 and 7, the advanced injection timing shows maximum peak heat release rate and maximum accumulated heat release and retarded timing shows lower peak heat release rate and lower accumulated heat release. It can be concluded, in the case of advanced injection timing, a large amount of evaporated fuel is accumulated resulting in longer ignition delay. The longer ignition delay leads to rapid burning rate and the pressure and temperature within the cylinder rises rapidly. The predicted amount of soot and NO<sub>x</sub> emissions compared to their experimental values at different injection timing is illustrated in Fig. 8.

Results shown in Fig. 8 indicate that the optimum operating point to gain the best NO<sub>x</sub>-soot trade-off could be obtained by injecting fuel at 0.65 CA BTDC. Moreover, the results confirm that there is a good conformity between the experimental and computational data, and this shows that the models used in this study has sufficient capacity to predict the operating conditions of the engine.

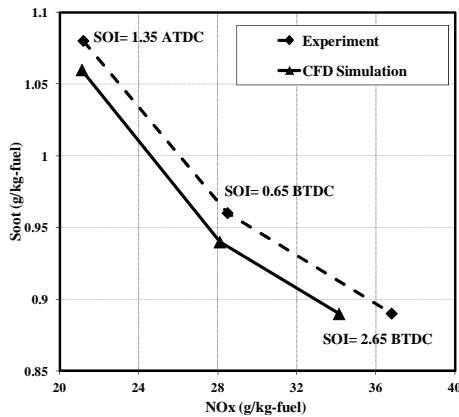


Fig. 8 Effect of the injection timing on NOx and soot emission

C. Combustion Chamber Optimization

Typically, high-speed direct injection (HSDI) diesel engines use a re-entrant combustion chamber. The re-entrant shape strongly affects the fuel distribution along the combustion chamber wall and air-fuel mixing and therefore affects the emissions and performance. Fig. 9 shows the schematic diagram of a re-entrant combustion chamber with the different geometry parameters which was analyzed in the present study.

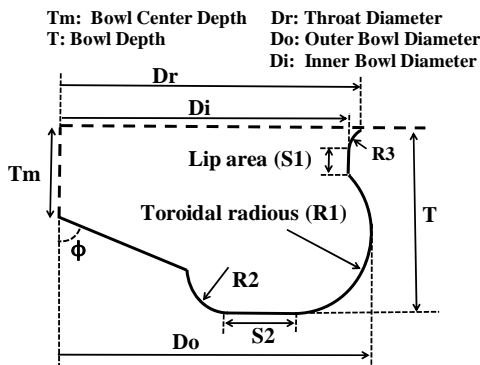


Fig. 9 A Re-Entrant combustion chamber

Totally, thirteen different combustion chambers have been selected to analyze the different geometrical parameters on engine performance and amount of pollutant emissions. The 7 parameters varied in the current optimization are listed in Table II, along with each parameter's range. The geometrical configurations of these models are shown in Fig. 10.

TABLE II  
LIST OF OPTIMIZATION PARAMETERS AND THEIR RANGES

Parameters	Range
Tm (mm)	4.52 - 7.52
T (mm)	12.42 - 16.42
Dr (mm)	45.20 - 51.20
Do (mm)	48.20 - 51.20
Di (mm)	43.56 - 49.56
S1 (mm)	1.46 - 5.46
S2 (mm)	3.3 - 9.3

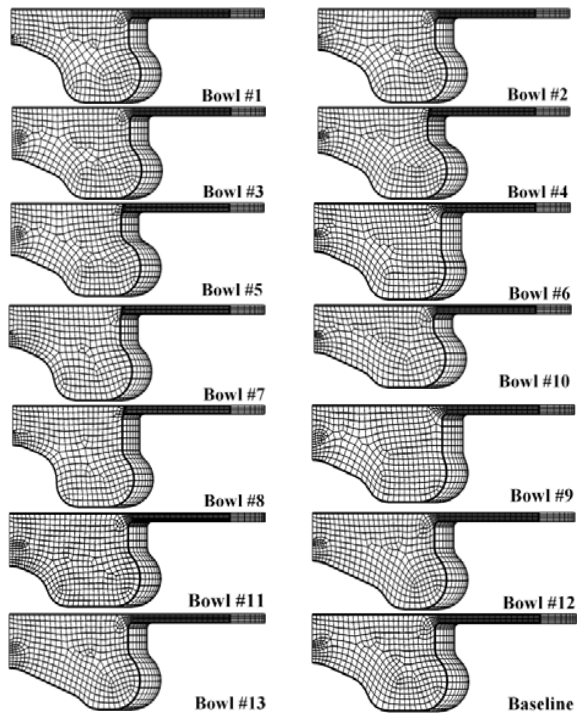


Fig. 10 Proposed combustion chamber configurations compared to the baseline case

As can be seen in Fig. 10, these models had a wide range of characteristics. It should be noted that although changes in geometry occur, grid resolution and quality remain unchanged for all investigated cases.

In area of piston design, it is very difficult to change one independent variable without effecting a change in another independent variable. When this is the case, the dependant variables will reflect the net effects of change in both independent variables. For this purpose, in three following sections, the effects of different geometry parameters has been classified and studied based on three categories including piston bowl depth, piston bowl width as well as piston bottom surface and lip area.

1. Piston Bowl Depth

One of the most dominant physical characteristics of the combustion chamber geometry is piston bowl depth. The effect of this parameter are presented and discussed in the following section.

In Fig. 11, the NOx emission is plotted as a function of piston bowl depth. For this investigation the bowl depth and bowl centre depth was changed from 12.42 to 16.42 mm and 4.52 to 7.52, respectively. It should be stated that in general, one piston design parameters cannot be changed without also changing other parameters. For example, in the piston depth study, to preserve compression ratio, either the squish high could be reduced as the piston bowl became deeper, or the piston bowl width could be decreases as the bowl become deeper.

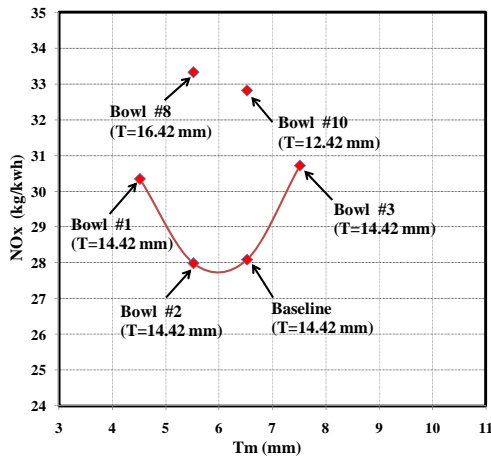


Fig. 11 Piston bowl depth effects on NOx emissions

As shown in Fig. 11, the Bowl #8 and Bowl #10 produce the highest NOx emission compared to other cases in this category. A slightly better operating condition has achieved with Bowl #2 which has the same bowl depth as baseline case while its bowl depth centre is lower than baseline case.

Fig. 12 plots the soot emissions of various models as a function of piston bowl depth. As can be seen in Fig. 12, the trend of soot emission is not as strong function of piston centre depth as previously discussed parameter, but soot still appears to decrease with increasing piston centre depth.

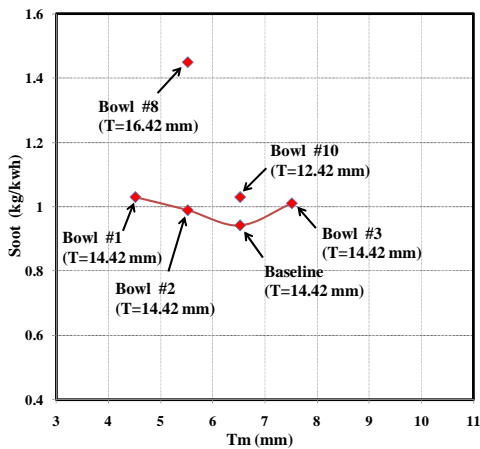


Fig. 12 Piston bowl depth effects on soot emissions

Fig. 13 shows the effect of piston bowl depth on brake specific fuel consumption.

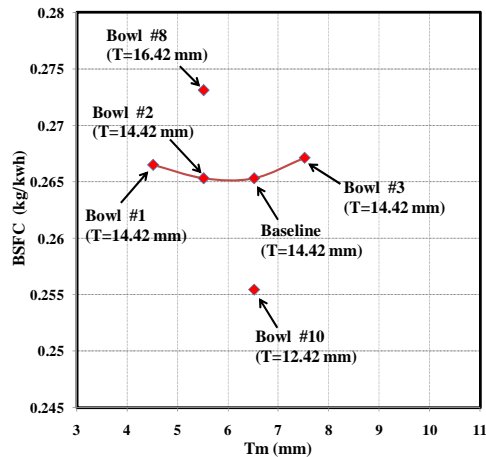


Fig. 13 Piston depth effects on BSFC

As illustrated in Fig. 13, the higher fuel consumption rate could be observed when the bowl depth is increased to 16.42mm (Bowl #8). In contrast, the best BSFC rate is achieved when the bowl depth is decreased to 12.42mm while the bowl centre depth (Tm) was the same to baseline case. It can be concluded that a deep bowl depth combined with a shallow bowl centre depth is disastrous for fuel economy.

2. Piston Bowl Width

To examine the effects of piston bowl width, the details results will be examined from three different bowls compared to the baseline case. In Fig. 14, the NOx is plotted as a function of piston depth. In these models, three geometrical parameters including bowl diameter, inner bowl diameter and outer bowl diameter have been considered to evaluate their effects on engine performance and amount of pollutants emissions.

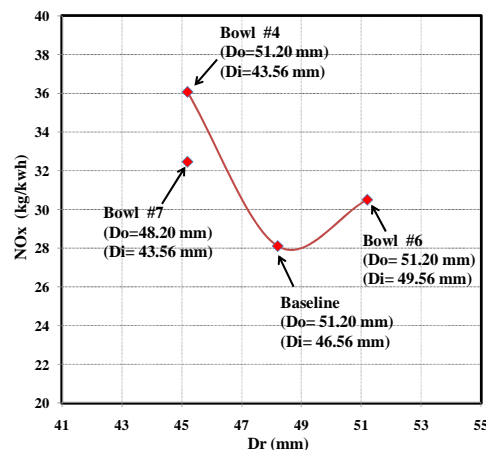


Fig. 14 Piston bowl width effects on NOx emission

Fig. 15 shows soot emissions as a function of piston bowl width.

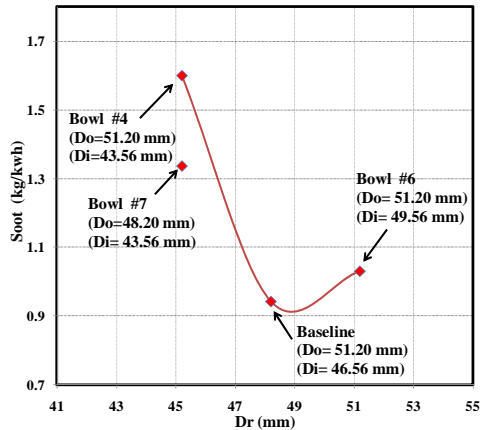


Fig. 15 Piston bowl width effects on soot emissions

As can be seen in Figs. 14 and 15, none of these three cases could improve the amount of NOx and soot emission compared to the baseline case. According to Figs. 14 and 15, increasing the bowl diameter till 48.2mm decreases the amount of NOx and soot emissions. After this point, the reverse trend has observed. It can be concluded, the narrower width have a higher unburned fuel air mixture region, and thus would have higher soot emissions. But with slightly wider combustion chamber the optimum operating point could be obtained.

Fig. 16 shows the effect of piston depth on brake specific fuel consumption.

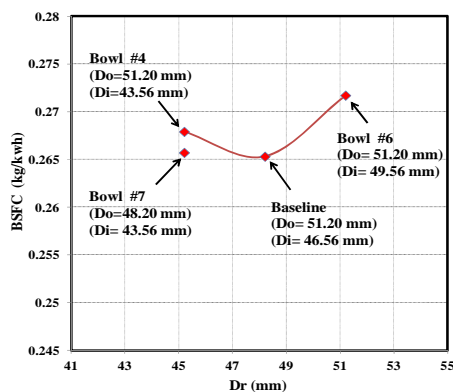


Fig. 16 Piston bowl width effects on BSFC

As illustrated in Fig. 16, the bowl #6 has the worst results, which indicates the wider bowls did not improve the fuel consumption.

### 3. Piston Bottom Surface and Lip Area

Another important parameter which has influence on design on re-entrant combustion chamber is bottom surface of the piston and also lip area of the bowl which has defined as S1 and S2 in Fig. 9. In this section the influence of these parameters are discussed. For this purpose, 5 different sketch of combustion chamber has simulated and analyzed compared to baseline case.

Figs. 17 and 18 show NOx and soot emissions as a function of piston bottom surface and lip area. As illustrated in Figs. 17 and 18, the worst operating point have been obtained by using Bowl #9 which has the highest lip area compared to other cases. It can be concluded that in the bowl with higher lip area, the spray impinges on the wall a little earlier than in the bowl with smaller lip area. Therefore the amount of fuel inside the bowl is larger than in the bowl with smaller lip area and this causes higher soot and NOx emissions.

The BSFC rate is plotted as a function of piston bottom surface and outer surface distance in Fig. 19.

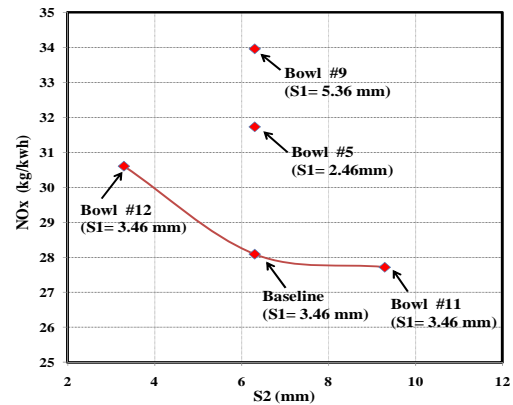


Fig. 17 Piston bottom surface and lip area effects on NOx emissions

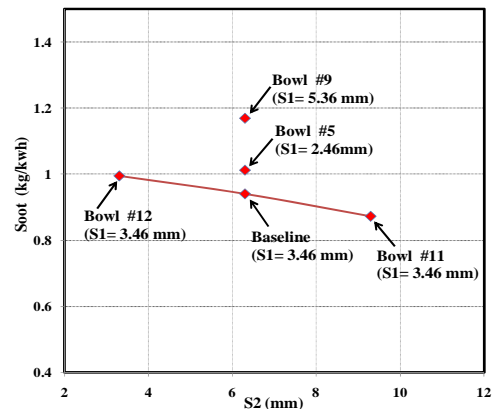


Fig. 18 Piston bottom surface and lip area effects on soot emissions

As can be seen in Fig. 19, Bowl #11 there appears to be a linear relationship between BSFC and piston bottom surface. As the piston bottom surface increases, the BSFC has a slight increasing when the lip area remains constant.

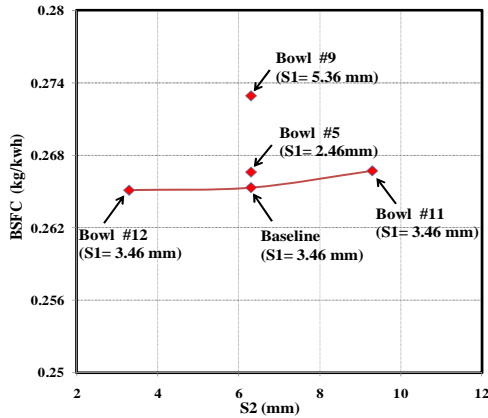


Fig. 19 Piston bottom surface effects on BSFC

Figs. 20 and 21 summarize the amount of CO emission and NO<sub>x</sub>-soot trade-off for all investigated cases, respectively.

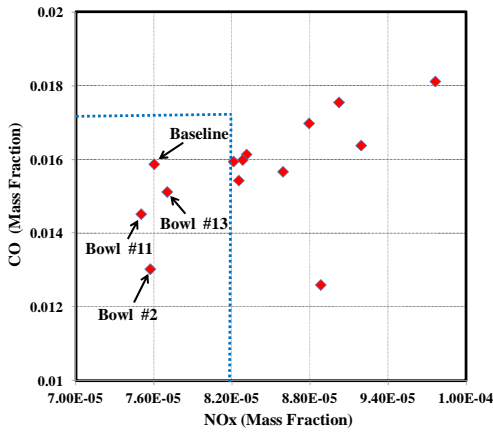


Fig. 20 NO<sub>x</sub> vs. CO for all studied cases

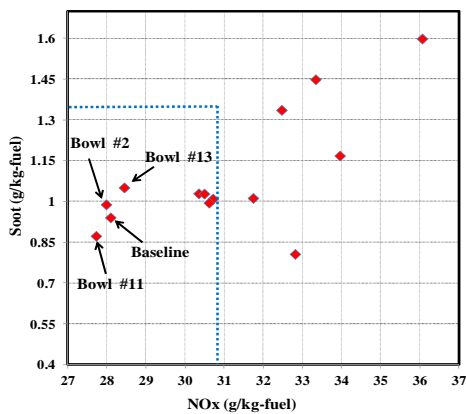


Fig. 21 NO<sub>x</sub> vs. Soot for all studied cases

As shown in Fig. 20, the two cases including the Bowl#11 and Bowl#12 have lower CO emissions compared to the baseline case. In addition, the Bowl #11 produced the best-soot trade-off point, as illustrated in Fig. 21.

*D. Optimum Models*

Based on results which have been obtained in previous sections, two configurations have been selected as optimum models to analyze in more detail.

Fig. 22 shows a comparison of pressure traces, heat release rates, and emissions between the baseline case and two optimum cases (Bowl #2 and #11).

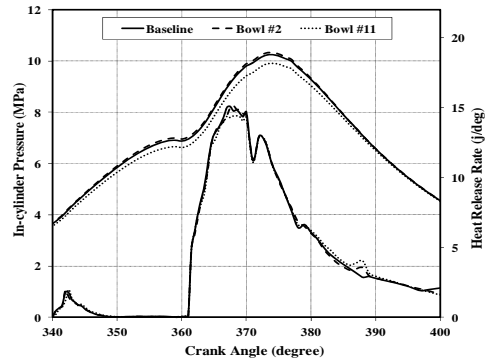


Fig. 22 In-cylinder pressure and heat release rate, baseline case vs. with two optimum cases

In Fig. 22, except for Bowl #11, the in-cylinder pressure and heat release rates are rather similar for the two other cases. Recall that the compression ratio was held constant for all geometries considered. As can be seen in Fig. 20, although the Bowl #11 has the lowest peak pressure, its heat release rate (HRR) trace implies that more late-cycle combustion occurs starting around 387 CA, which contributes more expansion work. Because of its lower peak pressure (corresponding to a lower mean temperature), the Bowl #11 also has the lowest NO<sub>x</sub> emission, as it was indicated in Fig. 18.

Fig. 23 presents the history of the overall turbulent kinetic energy (TKE) in the combustion chamber for the optimum cases compared to the baseline cases.

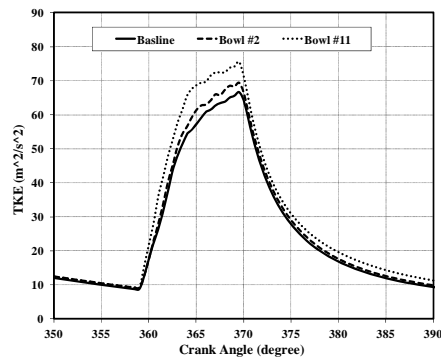


Fig. 23 Turbulent Kinetic Energy, baseline case vs. with two optimum cases

As shown in Fig. 23, after main fuel injection, the optimum cases' TKE raises to a level higher than that of the baseline case. This is mainly due to the much higher mixing rate of the optimum models.



Fig. 24 illustrates the velocity field contours for two optimum cases compared with the baseline case at 380 and 400 CA. As shown in Fig. 24, the velocity field within the cylinder increases for Bowl #11 and Bowl # 2 cases in comparison with the baseline case at 400 CA.

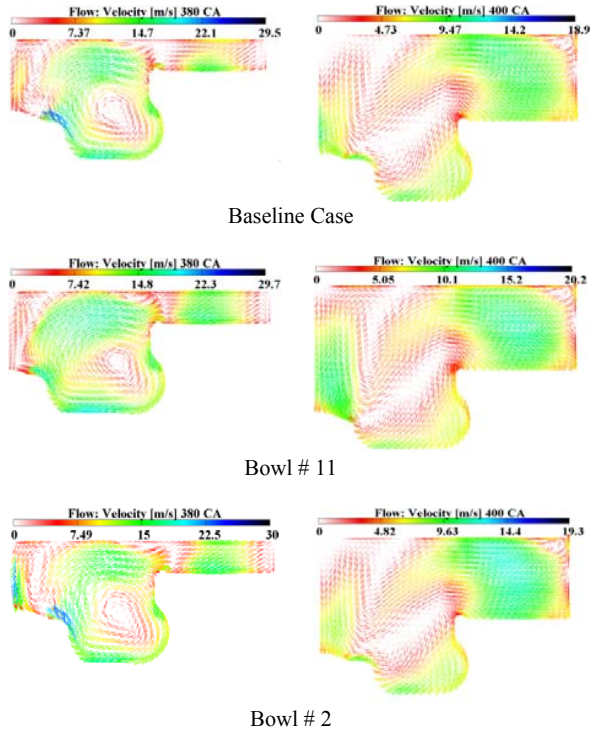


Fig. 24 The velocity fields contours, baseline case in comparison with two optimum cases

The evolution of the NOx distribution within the combustion chamber for the baseline case in comparison with optimum cases is shown in Fig. 25 at 380 and 400 CA. In addition, Fig. 26 shows the comparison of in-cylinder soot formations for the same operating points.

The local soot-NOx trade-off is evident in these contour plots, as the NOx formation and soot formation occur on opposite sides of the high temperature region. It can be seen that for the Bowl #11 case, has the lowest amount of NOx and soot mass fractions in comparison with other cases. It can be concluded that for this case, which has a larger bowl centre depth (Tm) than baseline case and Bowl #2, stronger squish flow has formed during the spray development and this increases the spray mixing with higher amount of velocity vectors.

The evolution of the CO emission for the baseline case compared with two other cases is illustrated in Fig. 27 at 380 and 400 CA.

As shown in Fig. 27, from 380 CA, the CO emissions distribution for Bowl#11 and Bowl#2 configurations is obviously smaller than baseline configuration. It can be concluded the later combustion in the exhaust stroke caused

this reduction although the burning velocity in the cylinder is nearly similar for three configurations at this position.

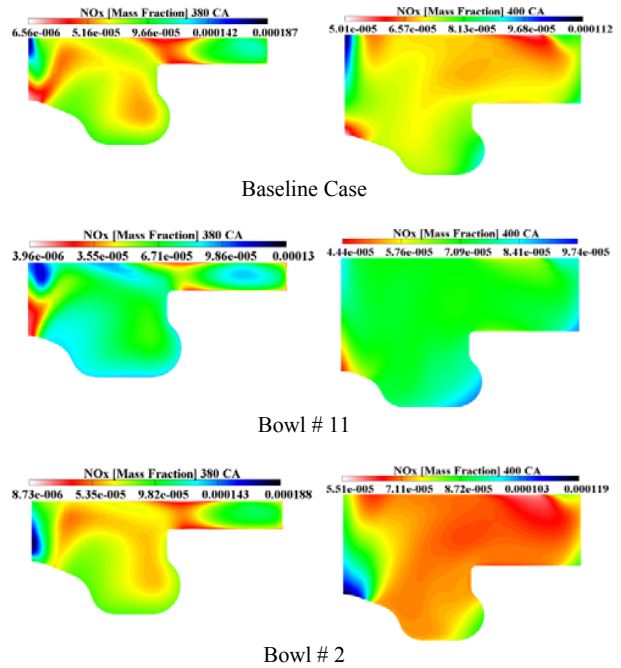


Fig. 25 The NOx contours, baseline case in comparison with two optimum cases

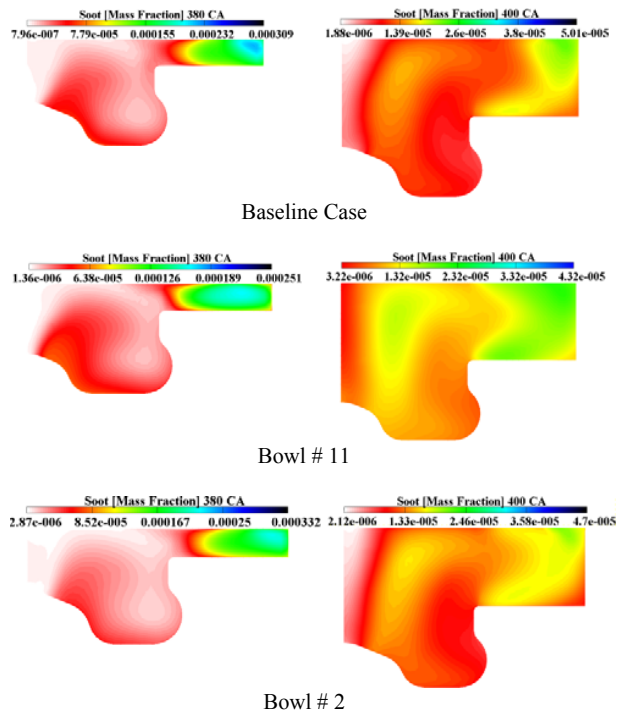


Fig. 26 The soot contours, baseline case in comparison with two optimum cases

*E. Effects of Pilot Injection Timing*

In order to further investigate the optimum geometries, the baseline pilot injection timings has been varied to evaluate its effects on amount of pollutant emissions and engine performance. For this purpose, the main injection was set at -0.65 CA ATDC and three pilot injection cases, with SOI -35, -25 and -20 CA ATDC are considered compared to the baseline injection case.

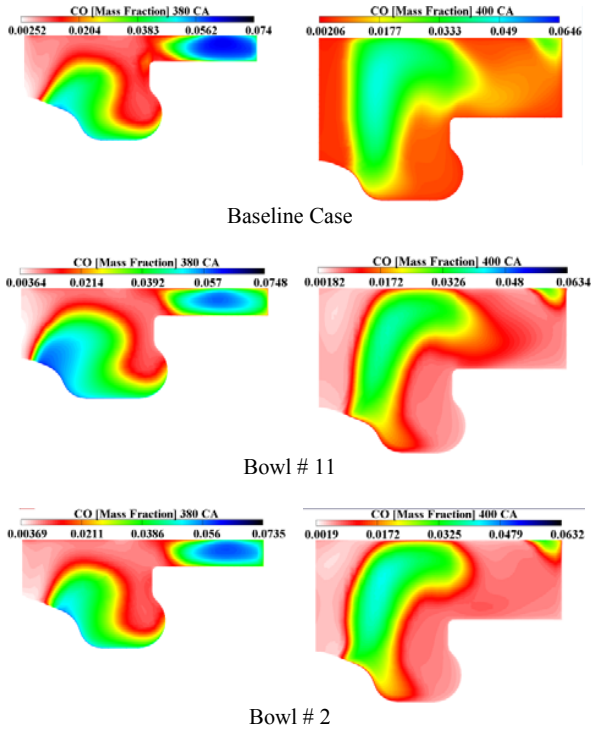


Fig. 27 The CO contours, baseline case in comparison with two optimum cases

In Fig. 28, the injection schemes used are illustrated schematically compared to the baseline injection case. It should be stated that the same amount of fuel is injected in all the studied cases.

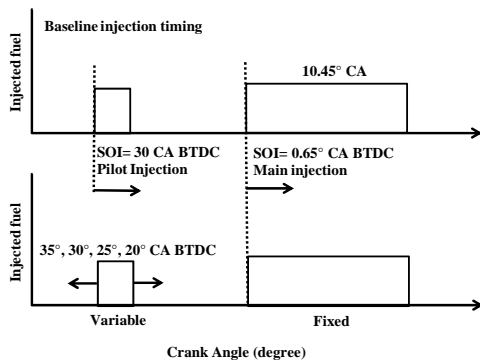


Fig. 28 Different pilot injection profiles compared to the baseline injection case

Figs. 29-31 show the amount of NOx, soot and BSFC for different considered cases, respectively.

The results in Figs. 28-30 demonstrate the NOx emissions could significantly decreased when the pilot injection timing was retarded to -25 CA BTDC while BSFC showed a slight increasing from 0.267 kg/kWh to 0.282 kg/kWh. In addition, since the soot oxidation was actively generated at higher combustion temperatures. Therefore, the amount of soot slightly increased as the injection timing was retarded.

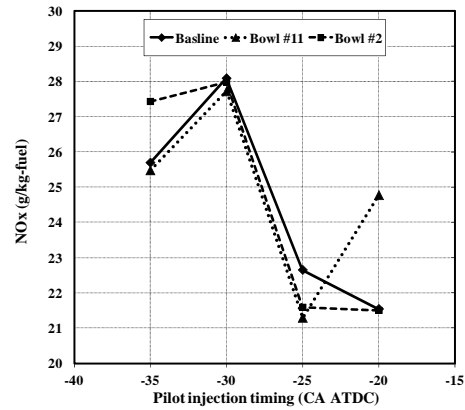


Fig. 29 NOx at different pilot injection timings for two optimum cases vs. the baseline case

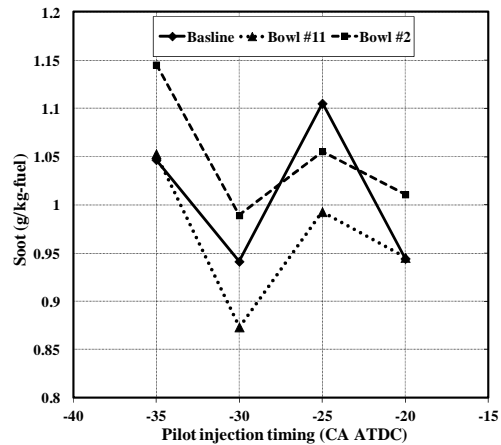


Fig. 30 Soot at different pilot injection timings for two optimum cases vs. the baseline case

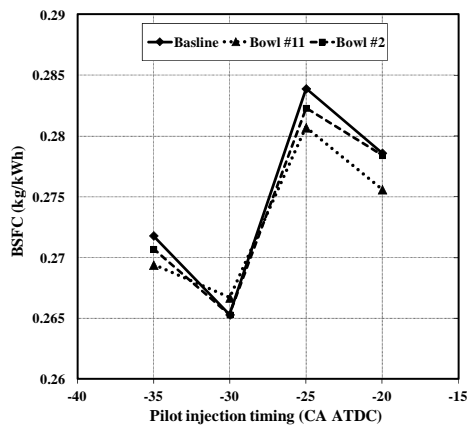


Fig. 31 BSFC at different pilot injection timings for two optimum cases vs. the baseline case

## VI. CONCLUSION

A CFD simulation was conducted to analyze the effects of combustion chamber geometry and pilot injection timing for optimization of engine performance and amount of pollutant emissions in a high speed direct injection (HSDI) diesel engine. The computed in-cylinder pressure, soot and NO<sub>x</sub> were firstly compared with experimental data under various ITs and good agreement between the predicted and experimental values was ensured the accuracy of the numerical predictions collected with the present work. To study the effects of combustion chamber geometry, thirteen different configurations were selected and analyzed compared to the original piston bowl geometry. The results showed that for shallower bowls, decreasing the bowl depth shows a higher amount of NO<sub>x</sub> emissions and a deep bowl depth combined with a shallow bowl centre depth is disastrous for fuel economy. It was also found that the narrower width of combustion chamber has a higher unburned fuel air mixture region, and thus would have higher soot emissions but with slightly wider combustion chamber the optimum operating point could be obtained. In addition, a potential has been found to improve the NO<sub>x</sub> emission compared to the baseline injection case while the engine's specific fuel consumption emissions remain approximately unchanged and soot formation could be slightly increased.

## REFERENCES

- [1] Cowland, C., Gutmann, P., and Herzog, P. L., "Passenger vehicle diesel engines for the U.S.", SAE Paper 2004-01-1452, 2004.
- [2] Pischinger, F. F. The diesel engine for cars – is there a future? Trans. ASME, J. Engng Gas Turbines Power, 1998, 120(3), 641–647.
- [3] Ge, H-W., Shi, Y., Reitz, R.D., and Willems, W., "Optimization of a high-speed direct-injection diesel engine at low-load operation using computational fluid dynamics with detailed chemistry and a multi-objective genetic algorithm", Proc. IMechE, Part D: J. Automobile Engineering, 2010, 224(4): 547-563.
- [4] Saito, T., Yasuhiro, D., Uchida, N., Ikeya, N., "Effects of Combustion Chamber Geometry on Diesel Combustion", SAE Paper 861186, 1986.
- [5] Bianchi, G.M., Pelloni, P., Corcione, F.E., Mattarelli, E., Luppino Bertoni, F., "Numerical Study of the Combustion Chamber Shape for Common Rail H.S.D.I. Diesel Engines", SAE Paper 2000-01-1179, 2000.
- [6] De Risi, A., Donato, T., Laforgia, D., "Optimization of the combustion of direct injection diesel engines", SAE Paper 2003-01-1064, 2003.
- [7] Zhu, Y., Zhao, H., Melas, D. A., and Ladommatos, N., "Computational study of the effects of the re-entrant lip shape and toroidal radii of piston bowl on a HSDI diesel engine's performance and emissions", SAE Paper 2004-01-0118, 2004.
- [8] Genzale, L. C. and Reitz, D. R., "Effects of Piston Bowl Geometry on Mixture Development and Late-Injection Low-Temperature Combustion in a Heavy-Duty Diesel Engine", SAE Paper 2008-01-1330, 2008.
- [9] Wickman, D.D., Yun, H. and Reitz, D., "Split-Spray Piston Geometry Optimization for HSDI Diesel Engine Combustion", SAE Paper 2003-01-0348, 2003.
- [10] Heywood, J. B., Internal Combustion Engine Fundamentals- Mc Graw-Hill New York, 1988.
- [11] Zhang, L., "A study of pilot injection in a DI diesel engine", SAE Paper 1999-01-3493, 1999.
- [12] Chen, SK., "Simultaneous reduction of NO<sub>x</sub> and particulate emissions by using multiple injections in a small diesel engine", SAE Paper 2000-01-3084, 2000.
- [13] Tanaka, T., Ando, A., Ishizaka, K., "Study on pilot injection of DI diesel engine using common rail injection system", JSAE Rev 2002; 23:297–302.
- [14] ICE Physics & Chemistry, AVL FIRE user Manual v.2009.2, 2009.
- [15] R. Tatschl, P. Priesching, J. Ruetz, "Recent Advances in DI-Diesel Combustion Modeling in AVL FIRE - A Validation Study", International Multidimensional Engine Modeling User's Group Meeting at the SAE Congress, Detroit, 2007.
- [16] R. Mobasher, Zhijun Peng and S. M. Mirsalim, "CFD Evaluation of Effects of Split Injection on Combustion and Emissions in a DI Diesel Engine", SAE 2011 World Congress, April 12-14, 2011, Cobo Center, Detroit, Michigan, USA, SAE Paper number: 2011-01-0822.
- [17] Hélie, J. & Trouvé, A., "A modified coherent flame model to describe turbulent flame propagation in mixtures with variable composition", Proc. Combust. Inst. 28, (2000): 193-201.
- [18] Colin, O., Benkenida, A., "The 3-Zones Extended Coherent Flame Model (ECFM3Z) for Computing Premixed / Diffusion Combustion", Oil & Gas Science and Technology – Rev. IFP, Vol. 59, No. 6, 2004, pp. 593-609.
- [19] Halstead, M., Kirsch, L. and Quinn, C., "The Auto Ignition of Hydrocarbon Fueled at High Temperatures and Pressures-Fitting of a Mathematical Model", Combustion Flame, Vol. 30, 45-60, 1977.
- [20] Reitz, R. D. "Modeling Atomization Processes in High-Pressure Vaporizing Sprays", Atomization and Spray Technology, Vol. 3: 309-337, 1987.
- [21] Naber, J.D. and Reitz, R.D., "Modeling Engine Spray/Wall Impingement", SAE Paper 880107, 1988.
- [22] Corcione, F. E., Allocca, L., Pelloni, P., Bianchi, G. M., and Luppino, F., "Modeling atomization and drop breakup of high-pressure Diesel Sprays", ASME Journal of Engineering for Gas Turbine and Power, Vol. 123, Issue 2, pp. 419-427, 2001.
- [23] Dukowicz, J.K., "Quasi-Steady Droplet Change in the Presence Of Convection", Informal Report Los Alamos Scientific Laboratory, LA7997-MS.
- [24] Han, Z. and Reitz, R. D., "Turbulence modelling of internal combustion engines using RNG k-ε models", Combust. Sci. and Technol., 1995, 106, 267–295.
- [25] Hiroyasu, H., and Nishida, K. "Simplified Three Dimensional Modeling of Mixture Formation and Combustion in a DI Diesel Engine", SAE Paper 890269, 1989.
- [26] Zhu, Y., Zhao, H., Melas, D. A., and Ladommatos, N., "Computational study of the effects of the geometry of piston bowl pip for a high-speed direct-injection diesel engine", Proc. IMechE, Part D: J. Automobile Engineering, 2004, 218, 875–890.